ISSN 2349-4506
Impact Factor: 2.785

Global Journal of Engineering Science and Research Management

EFFECT OF ADDING IRON-LOADED BIOCHAR ON STEAM GASIFICATION OF SUBBITUMINOUS COAL

Lingbo Shen*, Ayano Nakamura, Kenji Murakami

* Department of Engineering in Appied Chemistry, Faculty of Engineering and Resource Science, Akita University, 1－1 Tegata gakuen-machi, Akita city, Akita 010-8502 JAPAN

Department of Engineering in Appied Chemistry, Faculty of Engineering and Resource Science, Akita University, 1－1 Tegata gakuen-machi, Akita city, Akita 010-8502 JAPAN

Department of Engineering in Appied Chemistry, Faculty of Engineering and Resource Science, Akita University, 1－1 Tegata gakuen-machi, Akita city, Akita 010-8502 JAPAN

DOI: 10.5281/zenodo.253877

KEYWORDS: iron catalyst, coal, steam gasification, biochar, pyrolysis.

ABSTRACT

Iron-loaded woody biochar, which can be used as a catalyst and feedstock, was added to Indonesian Adaro sub-bituminous coal or coal char for steam gasification in a fixed-type reactor. This study aimed to determine the optimal content of added iron-loaded biochar for steam co-gasification in this system and the best time to add it. The amount of hydrogen evolution observed for the mixture of iron-loaded biochar and Adaro coal at 800 ºC was much higher than that observed for the mixture of iron-loaded biochar and coal char. The optimal ratio of iron-loaded Japanese cedar biochar to Indonesian Adaro subbituminous coal char was determined to be 1:1 by weight. X-ray diffraction patterns of the different mixtures after pyrolysis revealed that the iron catalyst contained in the iron-loaded biochar may affect the pyrolysis of Adaro coal. The mechanism by which the iron catalyst in iron-loaded biochar promoted the co-gasification reactivity was also discussed.

INTRODUCTION

In recent years, biomass has attracted substantial attention as a renewable resource because of the rapid exhaustion of fossil fuel reserves. Utilization of mixtures of biomass and coal has been considered an important and practical method of ameliorating the energy crisis [1–2]. Among methods of utilizing such biomass-coal mixtures, co-gasification has been widely researched. Co-gasification of biomass and coal can improve the reactivity and efficiency of gasification compared to the gasification of biomass or coal alone [3–5]. For example, Zhang et al. [6] conducted the CO_2 co-gasification of biomass (Chinese redwood or soybean stalk) and a bituminous coal from Ningxia in a fixed-bed reactor and reported that the durations required for the complete gasification of coal and soybean stalk (93 min) and coal and redwood (129 min) were 44 min and 8 min, respectively, shorter than that required for coal alone (137 min). These results indicated that stronger synergy can be achieved in the mixed-bed configuration than for the gasification of individual components. Wei et al. [7] studied the reactivity characteristics and synergy behaviors of the co-gasification of rice straw and bituminous coal and reported a close relationship between the synergy and transformation of K/Ca in biomass ash during the co-gasification process. Additional studies have revealed that some components of biomass, such as alkali and alkaline earth metals, act as catalysts of coal gasification during co-gasification processes [8–10]. This phenomenon is believed to be one of the main reasons underlying the improved gasification efficiency observed for the co-gasification of biomass and coal. However, wood, which is a type of biomass, has low contents of alkali and alkaline earth metals. In fact, some studies observed little synergy during the co-gasification of coal and wood [11–13]. Therefore, other catalysts are required to ensure high gasification efficiency in the co-gasification of woody biomass and coal. However, few studies have addressed the catalytic co-gasification of wood and coal. In our previous work, an iron-loaded biochar (produced by the pyrolysis of 7 wt% iron-loaded Japanese cedar [SG] at 800 °C) was mixed with Indonesian subbituminous coal at 20 wt%, and then, the mixed sample was gasified with steam at 800 °C for 60 min. The hydrogen evolution from this system was observed to increase by 20% compared to that observed for the steam gasification of coal alone in the presence of the same amount of iron catalyst. We also demonstrated that the small amount of alkali and alkaline earth metals contained in the biomass ash maintained the iron catalyst in an active state, even in the late stages of gasification; however, in the absence of an iron catalyst, these elements did not

promote the gasification of coal to the same degree [14]. Despite these results, two problems still require addressing. First, when the iron-loaded biochar should be added must be determined. Specifically, the question of whether the iron-loaded biochar should be mixed with the coal (i.e., before pyrolysis) or coal char (i.e., after pyrolysis) to obtain higher gasification efficiency must be resolved. Second, the mixing ratio of iron-loaded biochar and coal/coal char is believed to strongly affect the co-gasification efficiency [15–17]. In our previous study, only two mixed samples—10 wt% and 20 wt% iron-loaded biochar in coal—were gasified with steam. Therefore, the optimum mixing ratio needed to maximize the gasification efficiency in the co-gasification of iron-loaded biochar and coal/coal char remains to be identified [14].

The purpose of this study is to determine the optimum time for the addition of the iron-loaded biochar and the optimum mixing ratio of iron-loaded biochar to coal/coal char for co-gasification.

EXPERIMENTAL

Samples

Indonesian Adaro subbituminous coal (AD) was ground into a powder in a mortar. The AD particles used in the gasification experiment were allowed to pass through a 250-μm sieve but not through a 150-μm sieve. SG was used as the woody biomass and was cut into small pieces in a blender, ground into a powder in a mortar, and passed through a 250-μm sieve. The proximate and ultimate analyses of AD and SG are shown in Tables 1 and 2, respectively. All samples were dried at 110 °C for 1 h prior to use. The ash content was calculated as the residual amount after the calcination of 1 g of AD or SG at 815 °C for 1 h in air. The amount of volatile matter was determined based on the weight change before and after carbonization at 900 °C for 7 min. The fixed carbon content was obtained by subtracting the ash content (wt%) and the volatile matter content (wt%) from 100 wt%. The carbon, hydrogen, and oxygen contents were measured using an HCN recorder (Yanaco MT-700HCN), and the sulfur content was analyzed using an elemental analyzer (PerkinElmer 2400 II CHNS/O).

Iron catalyst loading

In this study, an impregnation method was used to deposit the iron salt onto the surface of SG. A weighed amount of SG (10 g) was immersed in 200 mL of aqueous solution containing $FeCl_2$, and the resulting suspension was stirred at 40 °C for 1 h under vacuum using a rotary evaporator. Then, the water was evaporated at 60 °C for 1 h. The impregnated samples were dried at 110 °C for 1 h prior to use. Iron catalyst loadings were determined by inductively coupled plasma mass spectrometry (SII SP5510). The samples prepared in this study were denoted as 7Fe-SG, where the numerical value in the sample name represents the iron loading (wt%).

Preparation of mixed samples of iron-loaded biochar and AD

The iron-loaded biochar was produced from 7Fe-SG. The samples (0.5 g) were heated from room temperature to 800 °C at a rate of 300 °C/min under flowing He gas (140 mL/min) and held at this temperature for 10 min. After cooling to room temperature, the iron-loaded biochars were preserved in nitrogen-purged polyethylene bags. These samples were designated as 7Fe-SGChar. The iron content in the 7Fe-SGChar was concentrated to 23 wt% because the sample weight decreased to approximately 30 wt% after pyrolysis.

The prepared iron-loaded biochar was added to AD at ratios of 1:10 to 10:10 and were named as follows: Fe-SGChar/AD (1:10) to Fe-SGChar/AD (10:10), respectively. To determine the effectiveness of iron-loaded biochar for co-gasification, the iron-loaded biochar was also added to ADchar. Because the yield of ADchar was roughly 50 wt%, the ratio of iron-loaded biochar to ADchar ranged from 1:5 to 10:5 to maintain the iron and carbon contents of Fe-SGChar/AD. These samples were named as follows: Fe-SGChar/ADchar (1:5) to Fe-SGChar/ADchar (10:5), respectively.

Pyrolysis and gasification

Fig. 1 shows the fixed-bed reactor used for the pyrolysis and gasification processes performed in this study. Initially, approximately 0.5 g of Fe-SGChar/AD or 0.25 g~0.3 g of Fe-SGChar/ADchar (chosen to maintain the height of the samples) was placed on quartz wool in the middle of the vertical fixed-bed-type reactor. The sample was heated from room temperature to 800 °C at a heating rate of 300 °C/min under flowing He gas (140 mL/min). The Fe-SGChar/AD was held at 800 °C for 10 min to remove any volatile components. Because Fe-SGChar/ADchar contains little volatile contents, this sample was heated to 800 °C but was not held at that

temperature.After cooling to room temperature, the samples were removed from the reactor. The char yield after pyrolysis was calculated using the following equation:

$$Y_{\text{Char}} = \frac{W_{\text{Char}}}{W_{\text{sample}}} \quad (1),$$

whereY_{Char} is the yield of char [wt%], W_{Char} is the weight of the residue after pyrolysis [g (ash and catalyst free)], and W_{sample} is the weight of the sample before pyrolysis [g (ash and catalyst free)].

Steam gasification was performed at 800 °C for 60 min by introducing 50 vol% of steam/He into the reactor immediately after the pyrolysis of the samples. The amount of steam was controlled by setting the temperature of the steam generator at 87 °C. The gasses (i.e., H_2, CO, CO_2, CH_4, C_2H_4, and C_2H_6) produced during steam gasification were determined by an online MicroGC instrument (Agilent Technologies MicroGC 3000A). The gas evolution rate was calculated using the following equation:

$$R = \frac{V_{\text{vol}}\% \times L}{22.4 \times m_{\text{char}}} \quad (2),$$

where R is the gas evolution rate [mmol/g-char·min]; L is the total gas flow rate [mL/min], which was measured by a flow meter every 10 min; m_{char} is the weight of the char [g], which was measured after pyrolysis; and V_{vol}% is the volume fraction of each produced gas measured by the MicroGC instrument. The carbon conversion was calculated using the following equation:

$$X_{\text{Carbon}} = \frac{C_{\text{gas}}}{C_{\text{Char}}} \quad (3),$$

whereX_{Carbon} is the carbon conversion [mol%] and C_{gas} is the molar content of carbon in the total gas [mol (ash and catalyst free)], determined as $C_{\text{gas}} = C_{\text{CO}} + C_{\text{CO2}} + C_{\text{CH4}} + 2C_{\text{C2H4}} + 2C_{\text{C2H6}}$ (i.e., the sum of the molar contents of all the carbon-containing gases). C_{Char} is the molar content of carbon that was originally contained in the pyrolyzed char (mol), which was assumed to be 100% carbon.

Characterization of the pyrolyzed char and gasified residue

The chemical form of the iron catalyst during pyrolysis and gasification was evaluated by X-ray powder diffraction (XRD; Rigaku, Ultima IV) with Ni-filtered CuKα radiation. The crystallite size of the iron catalyst was calculated using the Scherrerequation:

$$L = \frac{K\lambda}{\beta \cos\theta} \quad (4),$$

where$L$ is the crystallite size [Å],λ is the wavelength [Å],β isthe peak width at half-maximum intensity [rad], K is equal to 0.9, and θ is the diffraction angle [°].

RESULTS AND DISCUSSION

Effect of iron-loaded biochar on the gasification of AD

Fig. 2 shows the hydrogen evolution rates of Fe-SGchar/AD (1:10–10:10) and Fe-SGchar/ADchar (1:5–10:5) during steam gasification at 800 ºC. Here, the results of Fe-SGchar/AD (x:10) are compared with those of Fe-SGchar/ADchar (x:5), where x ranged from 1 to 10. As described above, this variation occurred because the weight of AD decreased to approximately 50 wt% after pyrolysis at 800 °C for 10 min. Based on the data shown in Fig. 2, it was determined that the hydrogen evolution rates were maximized at approximately 5 min and subsequently decreased gradually with increasing reaction time for all samples. Fe-SGchar/AD exhibited a higher hydrogen evolution rate than Fe-SGchar/ADchar for all ratios of Fe-SGchar addition. Table 3 shows the amounts of hydrogen evolution and carbon conversion for Fe-SGchar/AD (1:10~10:10) and Fe-SGchar/ADchar (1:5~10:5) during steam gasification at 800 °C for 60 min. From Table 3, it can be seen that both the carbon conversion and the amount of hydrogen evolution of Fe-SGchar/AD were always higher than those of Fe-SGchar/ADchar. Table 3 also presents the amount of hydrogen evolution calculated using the following equation (A (sum)):

$$A(\text{Sum}) = \frac{A(\text{Fe-SGchar}) \times m(\text{Fe-SGchar}) + A(\text{ADchar}) \times m(\text{ADchar})}{m(\text{Fe-SGchar}) + m(\text{ADchar})} \quad (5),$$

where*A*(Fe-SGchar) [mmol/g-char] and *A*(ADchar) [mmol/g-char] are the amounts of hydrogen evolution observed for Fe-SGchar alone and ADchar alone, respectively; and *m*(Fe-SGchar) [g, dacf] and *m*(ADchar) [g, dacf] are the weights of Fe-SGchar and ADchar, respectively. In this calculation, these weights(i.e., *m*(ADchar) and *m*(Fe-SGchar)) were set to be equal to those used for co-gasification. Similar to our previous results [14], the amount of hydrogen evolution occurring during steam co-gasification was higher than the sum of the amounts of hydrogen evolution produced by the individual gasification of Fe-SGchar and ADchar (*A*(Sum)) in all cases. The last column in Table 3 presents the incremental amounts of hydrogen evolution between the co-gasification and individual gasification determined using the following equation:

$$Increment\ (\%) = \frac{A(\text{co-gasification}) - A(\text{Individual})}{A(\text{Individual})} \times 100 \qquad (6),$$

where*A*(co-gasification) is the amount of hydrogen evolution during steam co-gasification, which is shown in the first column in Table 3. Based on these results, the increments for Fe-SGchar/AD (14–29%) were higher than those for Fe-SGchar/ADchar (2–13%).

Fig. 3 shows the relationship between the specific rate and carbon conversion. The specific rate, *R*s [1/h], was employed to investigate the change in the carbon conversion relative to the residual amount of carbon and was calculated using the following equation:

$$Rs = \frac{Rc}{Wsc} \qquad (7),$$

where*R*crepresents the rate of carbon conversion [mol%/h], and W_{SC} represents the molar amount of residual carbon in the char [mol%]. Below approximately 10% of carbon conversion, the difference in the specific rates was small, whereas above 10%, the specific rates for Fe-SGchar/AD were larger than those for Fe-SGchar/ADchar. Thus, the promoting effect obtained by mixing Fe-SGchar and AD was always greater than that achieved by mixing Fe-SGchar and ADchar.

Influence of addition ratio of Fe-SGchar

From Table 3, it can be seen that as the amount of Fe-SGchar added increased, both the carbon conversion and the amount of hydrogen evolution initially increased and subsequently decreased. More specifically, in the steam gasification of Fe-SGchar/AD at 800 °C for 60 min, the carbon conversion was maximized (71 mol%) when the mixing ratio was 5:10. In contrast, for Fe-SGchar/ADchar, the carbon conversion was maximized (59 mol%) when the mixing ratio was 5:5. Similar to the carbon conversion, the maximum amounts of hydrogen evolution for Fe-SGchar/AD and Fe-SGchar/ADchar—126 and 110 mmol/g-char, respectively—when the mixing ratios of Fe-SGchar to AD and to ADchar were 5:10 and 5:5 by weight, respectively. Because the weight of AD decreased to approximately 50 wt% during pyrolysis at 800 °C for 10 min, as described above, the weight ratio of 5:10 was considered to result in the highest promotting effect for the mixture of Fe-SGchar/AD.

Change in the form of iron during pyrolysis and steam gasification

Based on the carbon conversion and hydrogen evolution data, the optimal time for the addition of iron-loaded biochar was determined to be before the pyrolysis of AD, and the optimal mixing ratio of Fe-SGchar was determined to be 1:1 by weight. Thus, two questions remained to be answered: (1) Why is the amount of hydrogen evolution of Fe-SGchar/AD higher than that of Fe-SGchar/ADchar? (2) Why does the mixing ratio of 1:1 exert the best effect on steam co-gasification? To answer these questions, we investigated the changes of the form of iron during pyrolysis and steam gasification.

Fig. 4 shows the XRD patterns of the chars obtained after the pyrolysis of Fe-AD and Fe-SG. The major chemical form of iron species in all the samples was determined to be α-Fe. In addition, a small amount of austenite (Fe-C) was present in the Fe-AD car, and interestingly, diffraction peaks attributable to cementite (Fe_3C) were present in the Fe-SG char. Based on these results, Fe_3C or Fe-C was considered to be formed by the reaction of the iron catalyst with the volatile matter evolved during the pyrolysis of SG or AD, respectively. Figs. 5 and 6 present the XRD patterns of Fe-SGchar/ADchar (5:5) and Fe-SGchar/AD (5:10), respectively, pyrolyzed under various conditions. For Fe-SGchar/ADchar (5:5) (Fig. 5), almost no changes in the form of the iron catalyst (α-Fe and

Fe_3C) occur during pyrolysis. In contrast, after the pyrolysis of Fe-SGchar/AD (5:10) at 450°C, α-Fe had disappeared completely, and most of the iron species were present as Fe_3C (Fig. 6). These results are attributable to the reaction of α-Fe with the volatile matter evolved from AD to produce Fe_3C. The iron forms differed between Fe-AD (Fig. 4) and Fe-SGchar/AD (5:10) (Fig. 6) because of the presence of alkali and alkaline earth metals in Fe-SGchar. Pouret al. reported that the dispersion of iron catalyst improved when both alkali and alkaline earth metals were present [18]. Moreover, Fe_3C has been reported to form readily via the reaction of the highly dispersed α-Fe with carbon [19]. In fact, the crystallite size of α-Fe on Fe-SG (26 nm) was much smaller than that on Fe-AD (45 nm). As shown in Fig. 6, Fe_3C decomposed to form α-Fe above 700 °C. This change in the iron form is believed to occur via the following equation (R1), which was reported by Li [20]:

$$Fe_3C \rightarrow 3Fe+C \qquad (8).$$

The carbon formed according to this equation might be very unstable. Accordingly, because of its high reactivity, this carbon should be easily gasified with steam in the early stages of gasification, thereby increasing the hydrogen evolution rate in the early stages of gasification of Fe-SGchar/AD (5:10) relative to that observed for Fe-SGchar/ADchar (5:5), as shown in Fig. 2 (c), (d), and (e). In contrast, because of the availability of insufficient amounts of the catalyst or carbon from volatile matter, little Fe_3C could be generated; thus, the increases of Fe-SGchar/AD (1:10), Fe-SGchar/AD (2:10), and Fe-SGchar/AD (10:10) were not obvious (Fig. 2 (a), (b), and (f)). Fig. 7 presents the XRD patterns of various samples after 5, 30, and 60 min of gasification. For Fe-AD (Fig. 7(g)), the iron species had already transformed into iron oxides (FeO and Fe_3O_4) after 5 min of gasification. Subsequently, FeO disappeared, and only Fe_3O_4 remained in the char. In contrast, for Fe-SGchar/ADchar (Fig. 7(b), (d), and (f)), α-Fe and Fe_3C remained in the char after 5 min of gasification, and the oxidation of the iron catalyst was slower than that observed using Fe-AD. The alkali metals in Fe-SGchar have been reported to prevent the oxidation of the iron catalyst to some extent [14, 18]. Therefore, the activity of the iron catalyst in Fe-SGchar/ADchar was considered to be high, even in the later stages of gasification, relative to that of Fe-AD.

Furthermore, the iron catalyst in Fe-SGchar/AD remained in its reduced form longer than that in Fe-SGchar/ADchar. Fe-SGchar/AD and Fe-SGchar/ADchar differ in terms of whether Fe-SGchar exists during the pyrolysis of AD or not. Qi [21] reported that iron atoms could be inserted between the layers of hexagonal carbon planes produced during the pyrolysis of coal. In this study, the iron catalyst on the Fe-SGchar may have moved to the AD surface during pyrolysis and suppressed the formation of a stable carbon structure, such as a graphite-like structure. In contrast, when the mixture of Fe-SGchar and ADchar was gasified, the effect of the iron catalyst on the steam gasification of ADchar was considered to be small because the ADchar consists of carbons with low reactivities. Zhang [22] reported that alkali metals could move from biomass to the coal surface and weaken C-C bonds of coal char during pyrolysis. This is one reason why the reactivity of AD did not decrease. Therefore, Fe-SGchar/AD was believed to be more reactive than Fe-SGchar/ADchar because of the interactions between carbons and iron/alkali metals during the pyrolysis of the coal.

In addition, in this study, the highest amount of hydrogen evolution and the maximum char conversion were observed when the Fe-SGchar was mixed with AD or ADchar in weight ratios of 1:2 or 1:1, respectively. Because the iron catalyst and alkali and alkaline earth metals exert a promoting effect on gasification, the hydrogen evolution increases as the amount of Fe-SGchar added increases. However, one question remains unaddressed: Why did the amount of hydrogen evolution decrease when a large amount of Fe-SGchar was added? In fact, similar results have been observed previously. For example, Che et al. [23] reported that a mixing ratio of 1:1 resulted in the highest synergy during the steam gasification of a mixture of pine sawdust and lignite in air atmosphere at from 800 °C to 950 °C. Additionally, Yan et al. [24] obtained similar results for the air and steam co-gasification of two types of woody biomass with brown coal at temperatures ranging from 700 °C to 900 °C. These authors attributed their results to the very low melting temperature of biomass ash: As a result, a large amount of biomass ash would cover the surface of the coal char, thereby blocking the pores of the coal char and limiting the contact between the coal char and the gasification agent. Although the biomass used in this study generated less ash, as the amount of biomass increased and the amount of ADchar decreased, a similar interaction between Fe-SGchar and ADchar may have occurred in our experiment. Qi [25] also investigated the relationship between iron loading and gasification reactivity and reported that a limit for the iron-loading amount exists and that, when this limit is exceeded, the gasification reactivity actually decreases. Our experiment may have been

affected by a similar phenomenon because the addition of large amounts of Fe-SGchar resulted in high iron-loading for AD. This may reasonably explain the decreased hydrogen evolution observed when large amounts of Fe-SGchar were added.

CONCLUSION

In this study, mixtures of iron-loaded biochar (the pyrolysate of iron-loaded biomass) and AD coal/ADchar with different weight ratios were gasified with steam at 800 ºC in a fixed-bed-type reactor. The conclusions obtained from this work are as follows:

1) The optimal time to add iron-loaded biochar in this co-gasification system is before the pyrolysis of AD, and the optimal ratio for the addition of Fe-SGchar to ADchar is 1:1 by weight.
2) Based on the relationships between the specific rate and carbon conversion obtained,the specific rate of Fe-SGchar/AD was always higher than that of Fe-SGchar/ADchar.
3) According to the XRD patterns of chars pyrolyzed at various temperatures, a transition between α-Fe and Fe_3C occurred in Fe-SGchar/AD but not in Fe-SGchar/ADchar and produced a large amount of highly reactive carbons. Additionally, the XRD patterns of chars gasified at 800 °C for various times revealed that the iron catalyst can be maintained in its reduced form on both Fe-SGchar/AD and Fe-SGchar/ADchar for a longer time than that on Fe-AD. Finally, the oxidation of Fe-SGchar/AD was delayed compared to that of Fe-SGchar/ADchar in the presence of the same amount of iron catalyst.

REFERENCES

1. Zheng YH, Li ZF, Feng SF, Lucas M, Wu GL, Li Y, Li CH, Jiang GM. Biomass energy utilization in rural areas may contribute to alleviating energy crisis and global warming: A case study in a typical agro–village of Shandong, China. Renewable and Sustainable Energy Reviews 2010; 14: 3132–3139.
2. Mun TY, Tumsa TZ, Lee U, Yang W. Performance evaluation of co–firing various kinds of biomass with low rank coals in a 500 MWe coal–fired power plant. Energy 2016; 115: 954–962.
3. Tursun Y, Xu S, Wang C, Xiao Y, Wang G. Steam co–gasification of biomass and coal in decoupled reactors. Fuel Processing Technology 2016; 141: 61–67.
4. Sjöström K, Chen G, Yu Q, Brage C, Rosén C. Promoted reactivity of char in co–gasification of biomass and coal: Synergies in the thermochemical process. Fuel 1999; 78: 1189–1194.
5. Pan YG, Velo E, Roca X, Manyà JJ, Puigjaner L. Fluidized–bed co–gasification of residual biomass/poor coal blends for fuel gas production. Fuel 2000; 79: 1317–1326.
6. Zhang Y and Zheng Y. Co–gasification of coal and biomass in a fixed bed reactor with separate and mixed bed configurations. Fuel 2016; 183: 132–138.
7. Wei JT, Guo QH, Chen HD, Chen XL, Yu GS. Study on reactivity characteristics and synergy behaviours of rice straw and bituminous coal co–gasification. Bioresource Technology 2016; in press.
8. Yu MM, Masnadi MS, Grace JR, Bi XT, Lim C.J., Li Y. Co–gasification of biosolids with biomass: thermogravimetric analysis and pilot scale study in a bubbling fluidized bed reactor. Bioresource Technology 2015; 175: 51–58.
9. Masnadi MS, Grace JR, Bi XT, Lim CJ, Ellis N. From fossil fuels towards renewables: inhibitory and catalytic effects on carbon thermochemical conversion during co–gasification of biomass with fossil fuels. Applied Energy 2015; 140: 196–209.
10. Nemanova V, Araz A, Truls L, Klas E. Co–gasification of petroleum coke and biomass. Fuel 2014; 117; 870–875.
11. Collot AG, Zhuo Y, Dugwell DR, Kandiyoti R. Co–pyrolysis and co–gasification of coal and biomass in bench–scale fixed bed and fluidized bed reactors. Fuel 1999; 78: 667–679.
12. Kumabe K, Hanaoka T, Fujimoto S, Minowa T, Sakanishi K. Co–gasification of woody biomass and coal with air and steam. Fuel 2007; 86: 684–689.
13. Aigner I, Pfeifer C, Hofbauer H. Co–gasification of coal and wood in a dual fluidized bed gasifier. Fuel 2011; 90: 2404–2412.
14. Shen L and Murakami K. Steam co–gasification of iron–loaded biochar and low–rank coal. International Journal of Energy Research 2016; 40: 1846–1854.
15. Howaniec N and Smolinski A. Effect of fuel blend composition on the efficiency of hydrogen–rich gas production in co–gasification of coal and biomass. Fuel 2014; 128: 442–450.

16. Yuan S, Dai Z, Zhou Z, Chen X, Yu G, Wang F. Rapid co–pyrolysis of rice straw and a bituminous coal in a high–frequency furnace and gasification of the residual char. Bioresource Technolodge2012; 109: 188–197.
17. Jeong HJ, Sang SP, Hwang J. Co–gasification of coal–biomass blended char with CO2 at temperatures of 900–1100 °C. Fuel 2014; 116: 465–470.
18. Pour AN, Shahri SMK, Bozorgzadeh HR, Zamani Y, Tavasoli A, Marvast MA. Effect of Mg, La and Ca promoters on the structure and catalytic behavior of iron-based catalysts in Fischer–Tropsch synthesis.Applied Catalysis A: General 2008; 348: 201–208.
19. Zhang J, Yin J, Cao W, Yang L. Characterization of ultrafine particle iron–carbide catalyst and investigation on the catalytical mechanism for F–T synthesis. Journal and fuel chemistry and Technology 1993; 21: 375–379.
20. Li X, Hui H, Li S, He L, Cui L. Integration of coal pyrolysis process with iron ore reduction: Reduction behaviors of iron ore with benzene–containing coal pyrolysis gas as a reducing agent. Chinese Journal of Chemical Engineering 2016; 24: 811–817.
21. Qi X, Guo X, Luo Z, Zheng C. Effect of Iron on the Structure of Shenfu Brown Coal Char During Pyrolysis. Journal of Engineering Thermophysics 2014; 4: 796–800.
22. Zhang Y, Zheng Y, Yang M, Song Y. Effect of fuel origin on synergy during co-gasification of biomass and coal in CO2. Bioresource Technology 2016; 200: 789–794.
23. Che D, Li J, Li S, Wang Q. Experimental Investigation of Effect of Biomass Blending Ratio on Coal Gasification. Characteristics Proceedings of the CESS 2013, 33: 35–40.
24. Yan W, Lu X. Investigation of Effect of the Blending Ratios of Biomass and Lignite on Characteristic of Co-gasification. Proceedings of the CSEE2009, 29: 150－155.
25. Qi XJ, Guo X, Xue LX, Zheng CG. Effect of iron on Shenfu coal char structure and its influence on gasification reactivity. Journal of Analytical and Applied Pyrolysis 2014, 110: 401–407.

Table 1. Proximate and ultimate analyses of Indonesian Adaro subbituminous coal(AD).

Prox. Analysis, wt% (dry)		Ultimate Analysis, wt% (daf)				
Ash	VM	C	H	N	S	O(diff.)
2.5	46.7	67.8	5.1	0.44	0.14	26.5

Table 2. Proximate and ultimate analyses of Japanese Cedar (SG).

Proxmate, wt% (dry)			Ultimate, wt% (daf)			
Ash	VM	FC	C	H	N	O(diff)
0.9	78.4	20.7	46.9	5.8	0.1	46.2

Table 3. Carbon conversion and amount of hydrogen evolution.

	Carbon conversion (mol%)	Amount of hydrogen evolution		
		Co-gasification（mmol/g-char）	Individual（mmol/g-char）	Increment (%)
Fe-SGchar/AD(1:10)	61	107	91	17.5
Fe-SGchar/ADchar(1:5)	49	93		2.2
Fe-SGchar/AD(2:10)	63	113	94	20.2
Fe-SGchar/ADchar(2:5)	51	98		4.3
Fe-SGchar/AD(4:10)	65	124	97	27.8
Fe-SGchar/ADchar(4:5)	58	107		10.3
Fe-SGchar/AD(5:10)	71	126	98	28.5
Fe-SGchar/ADchar(5:5)	59	110		12.2
Fe-SGchar/AD(6:10)	65	121	99	22.2
Fe-SGchar/ADchar(6:5)	55	106		4.1
Fe-SGchar/AD(10:10)	64	119	104	14.4
Fe-SGchar/ADchar(10:5)	56	107		2.9

ISSN 2349-4506
Impact Factor: 2.785

Global Journal of Engineering Science and Research Management

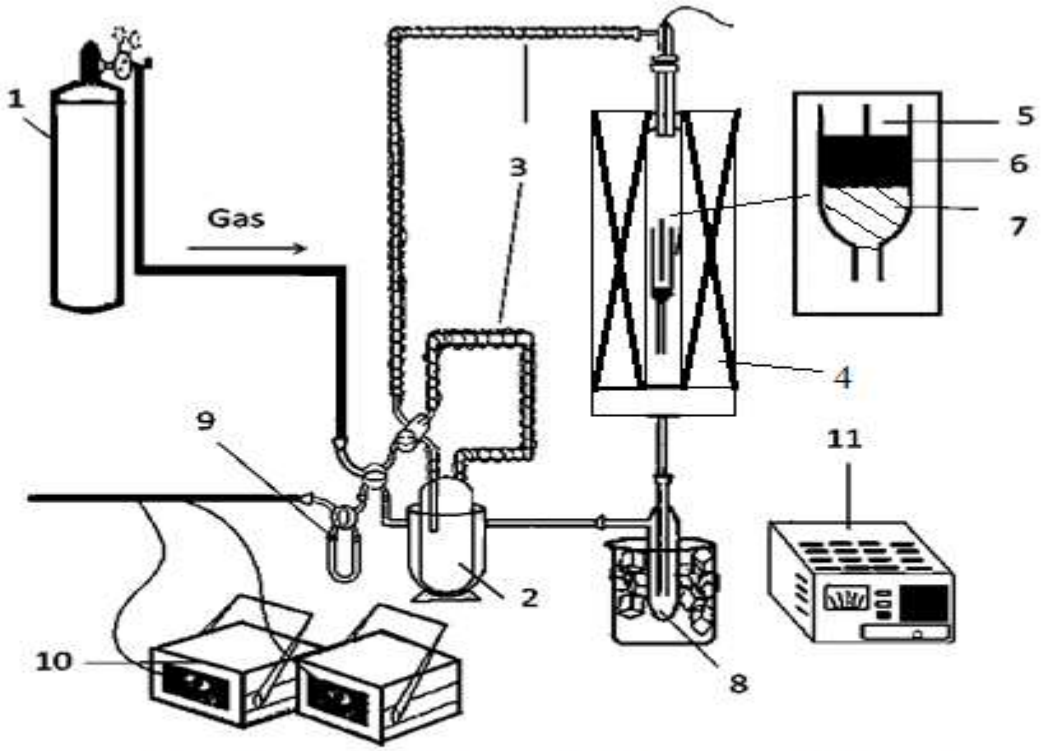

1. Carrier gas, 2. Steam generator, 3. Ribbon heater, 4. Electric furnace,
5. Thermocouple, 6. Sample, 7. Quartz wool, 8. Tar trap,
9. Dehydrating agent, 10. MicroGC, 11. Temperature controller

Figure 1. Fixed bed reactor for pyrolysis and steam gasification

ISSN 2349-4506
Impact Factor: 2.785

Global Journal of Engineering Science and Research Management

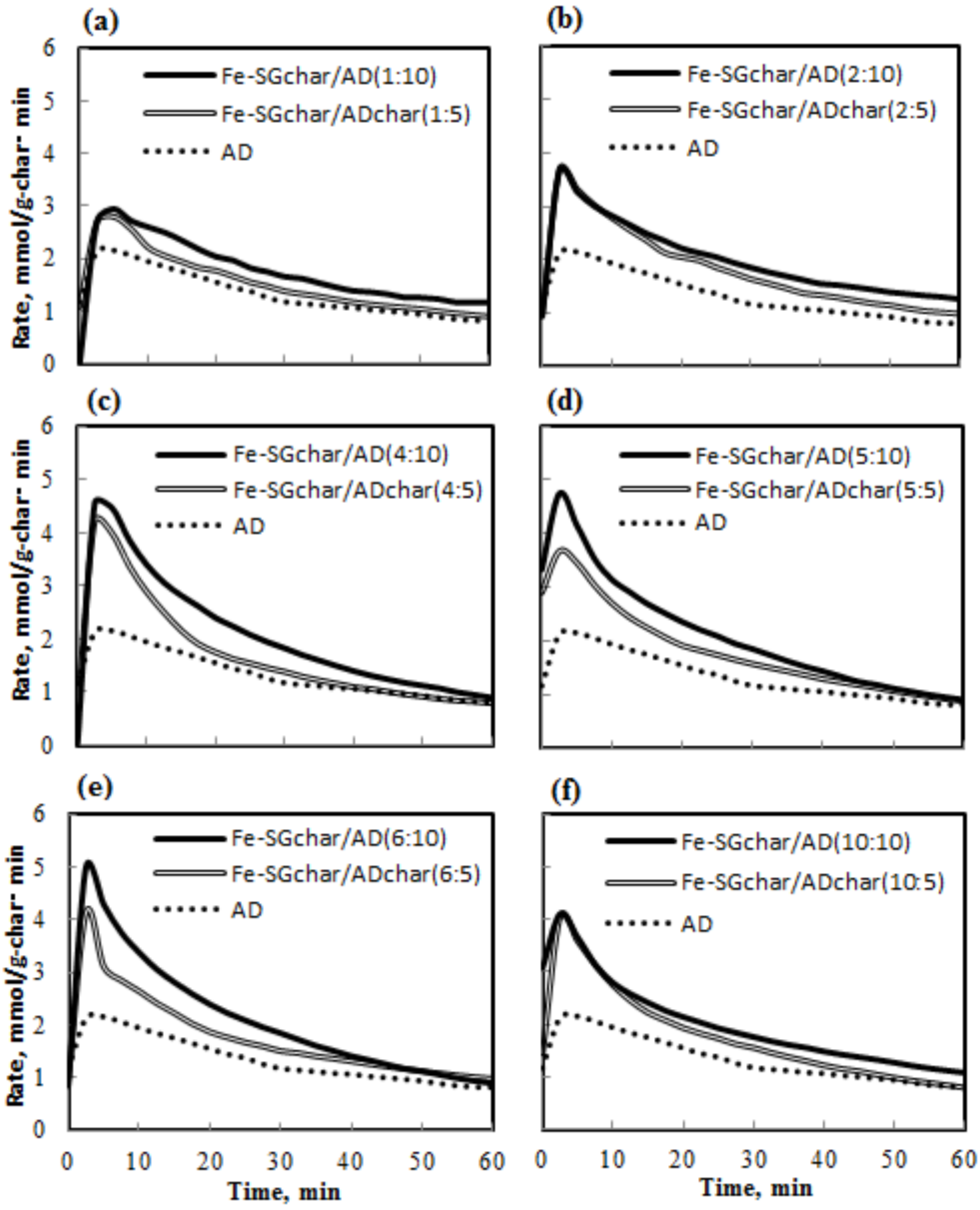

Figure 2. The H_2 evolution rate for Fe-SGchar/AD and Fe-SGchar/ADchar in different ratios

ISSN 2349-4506
Impact Factor: 2.785

Global Journal of Engineering Science and Research Management

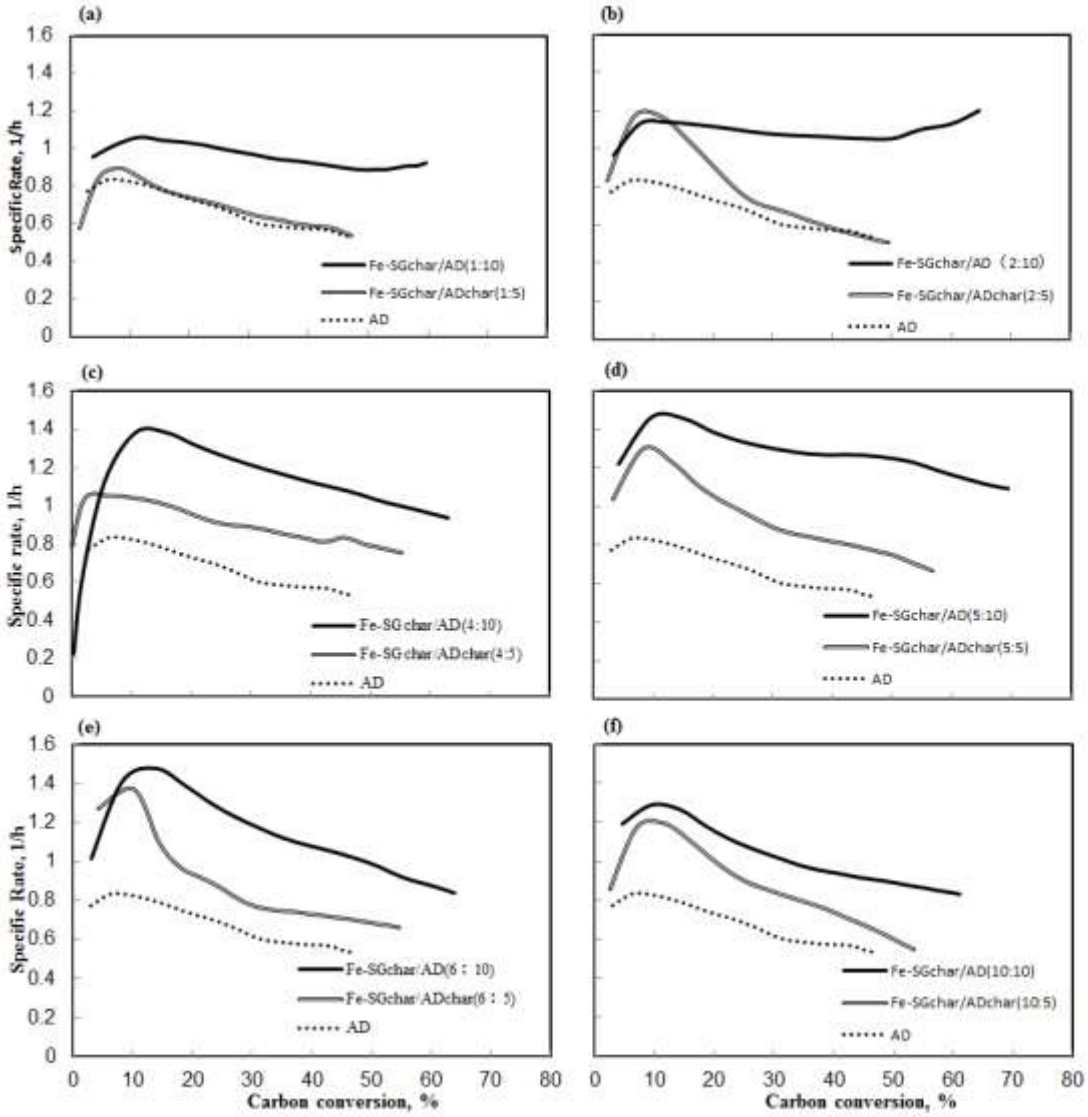

Figure 3. The relationship between specific rate and carbon conversion

ISSN 2349-4506
Impact Factor: 2.785

Global Journal of Engineering Science and Research Management

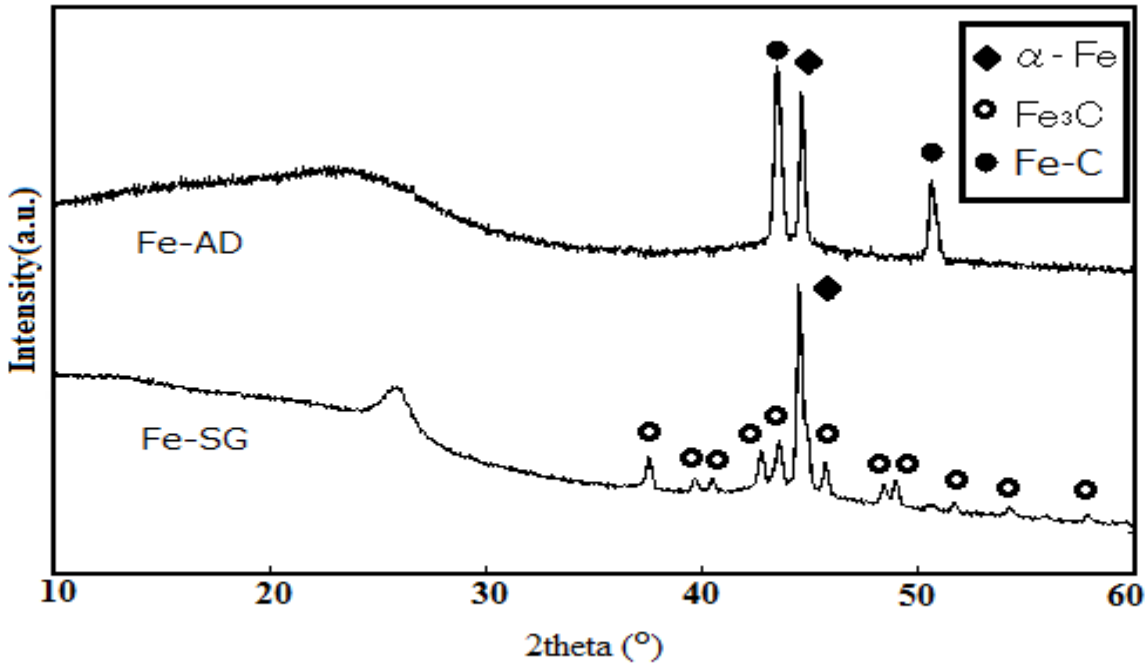

Figure 4. The XRD patterns of char after pyrolysis

ISSN 2349-4506
Impact Factor: 2.785

Global Journal of Engineering Science and Research Management

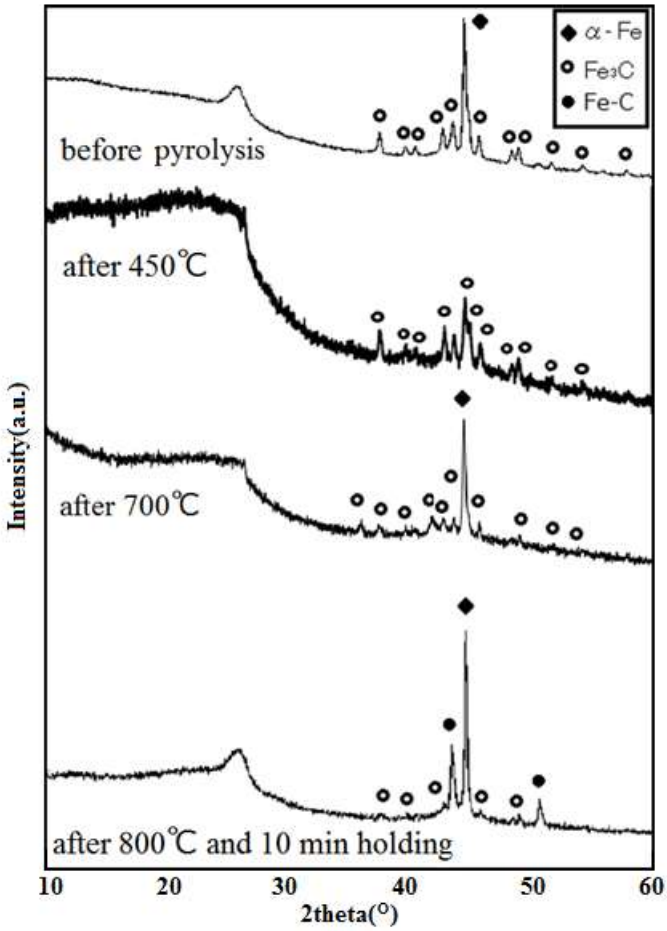

Figure 5. The XRD patterns of Fe-SGchar/AD (5:10) with temperature rising in the processing of pyrolysis

ISSN 2349-4506
Impact Factor: 2.785

Global Journal of Engineering Science and Research Management

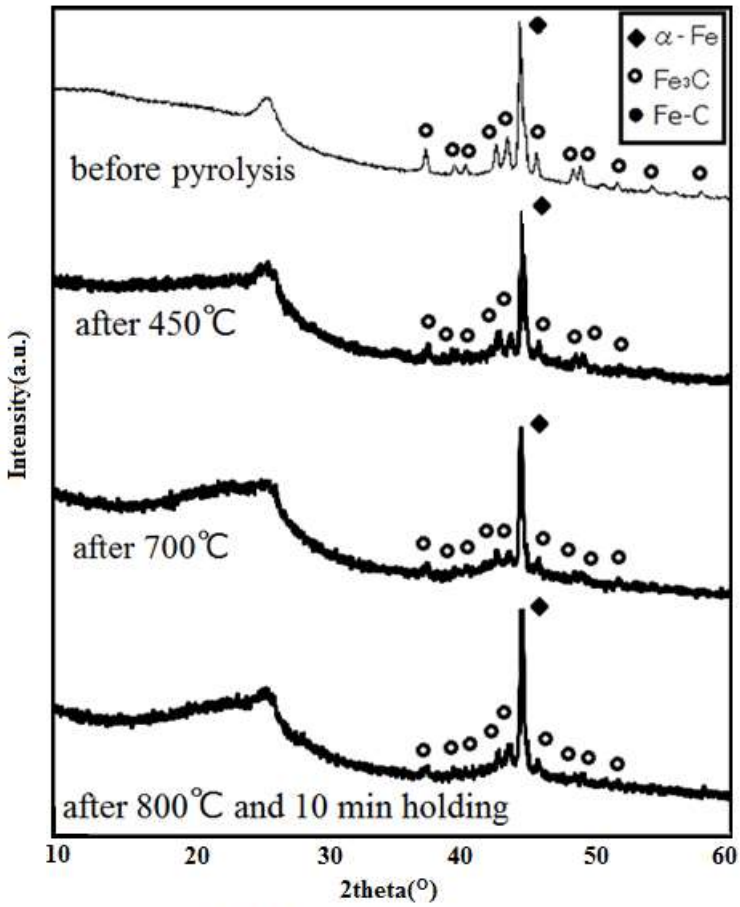

Figure 6. The XRD patterns of Fe-SGchar/ADchar (5:5) with temperature rising in the processing of pyrolysis

ISSN 2349-4506
Impact Factor: 2.785

Global Journal of Engineering Science and Research Management

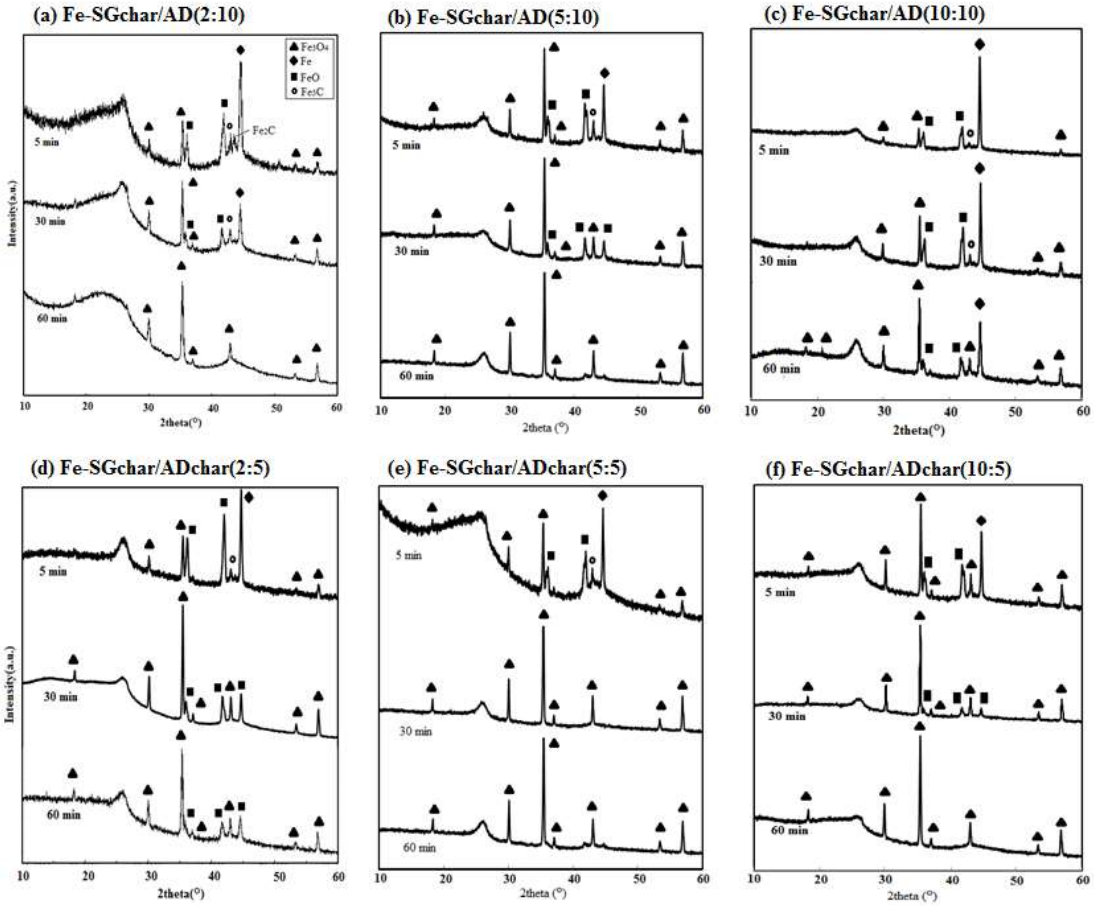

Figure 7(a). XRD patterns of Fe-SGchar/AD and Fe-SGchar/ADchar in and after gasification

ISSN 2349-4506
Impact Factor: 2.785

Global Journal of Engineering Science and Research Management

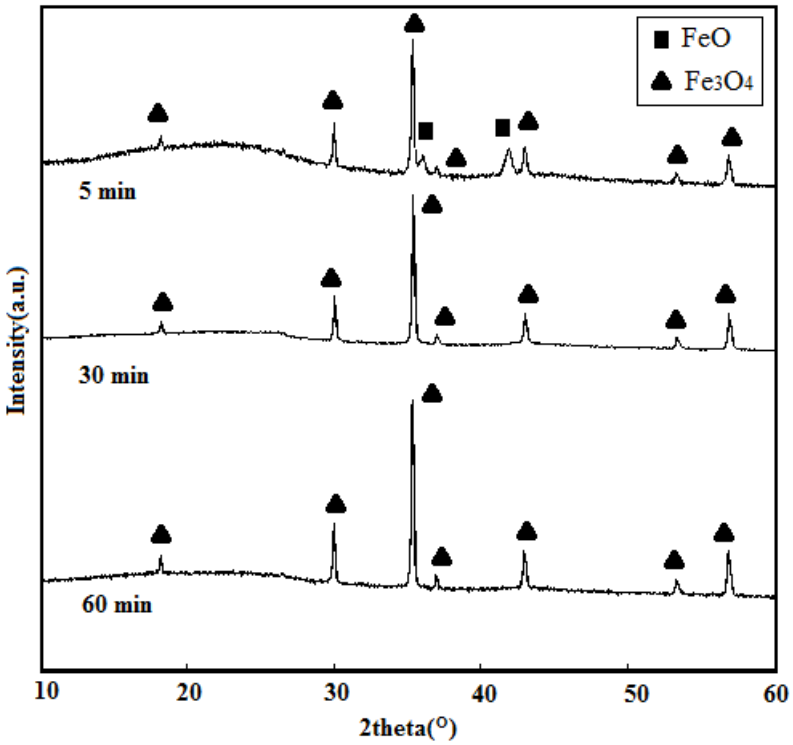

Figure 7(b). XRD patterns of Fe-AD in and after gasification